FIFTEEN YEARS OF HYPERSPECTRAL DATA: NORTHERN GRAPEVINE MOUNTAINS, NEVADA

F. A. Kruse and J. W. Boardman
Analytical Imaging and Geophysics LLC
4450 Arapahoe Ave, Suite 100
Boulder, Colorado, USA, 80303, kruse@aigllc.com

And

J. F. Huntington
Mineral Mapping Technologies Group
CSIRO Exploration and Mining
North Ryde, NSW, 2113, Australia

1.0 INTRODUCTION

The northern Grapevine Mountains (NGM) site, located in south-central Nevada (Figure 1), was designated part of a U.S. Geological Survey Wilderness Study Area in 1982. The USGS was charged with evaluating the economic mineral potential of the area by characterizing the surface geology, alteration, geologic structure, and existing prospects and claims. Remote sensing technology available at the time (Landsat MSS and TM data) was also used as part of this evaluation. Based on alteration mineralogy at the site, an airborne survey using Geophysical and Environmental Research's (GER's) 64 channel airborne spectral profiler was also flown. Results from the remote sensing analysis, field mapping and field spectral measurements, laboratory analyses, and ancillary data led to removal of the site from consideration as a WSA in 1984 (Wrucke et al., 1984).

Figure 1: Location map

Because the site was relatively well understood and mapped, repeated overflights of the NGM site with a variety of remote sensing instruments were arranged from 1984 through 1998 to evaluate remote sensing technology for resource assessment and to develop advanced analysis methodologies. Remote Sensing data available for the NGM site include Landsat MSS and TM, Thermal Infrared Multispectral Scanner (TIMS), JPL Airborne Synthetic Aperture Radar (AIRSAR) and SIR-C. Imaging spectrometer (hyperspectral) data flown for the NGM site include GER Spectral Profiler (1982), Airborne Imaging Spectrometer (AIS) (1984 - 1986), Airborne Visible/Infrared Imaging Spectrometer (AVIRIS) (1987, 1989, 1992, 1994, 1995), and Low Altitude AVIRIS (1998).

2.0 GEOLOGY

The main portion of the area mapped during this study (the NGM study area, Figure 1) consists of about one third of the "West of Gold Mountain" U.S. Geological Survey 7 1/2 minute quadrangle (1:24,000 scale). The site has been studied in detail using field mapping and several remote sensing data sets (Kruse, 1988, Kruse et al., 1993a). Some relatively detailed (1:62,500 scale) mapping has also been done in this area as part of U. S. Geological Survey Wilderness Assessment (WSA) Programs (Wrucke et al., 1984). Additional mapping of surficial deposits has been done at 1:62,500 scale (Moring, 1986). PreCambrian bedrock in the NGM area consists of limestones, dolomites, sandstones and their contact metamorphic equivalents, however, published geologic maps do not distinguish between the different lithologies. Mesozoic plutonic rocks are mapped primarily as granitic-composition and some age-dates are available (Albers and Stewart, 1972). Mesozoic units mapped in the field as part of this research include quartz syenite, a quartz monzonite porphyry stock, quartz monzonite dikes, and a granite intrusion (Figure 2) (Kruse, 1987). These rocks are cut by narrow north-trending mineralized shear zones containing sericite (fine grained muscovite or illite) and iron oxide minerals (Wrucke et al., 1984; Kruse, 1987). Slightly broader northwest-trending zones of disseminated quartz, pyrite, sericite, chalcopyrite, and fluorite mineralization (QSP alteration) ± goethite occur in the quartz monzonite porphyry. This type of alteration is spatially associated with fine-grained quartz monzonite dikes (Kruse, 1987). There are several small areas of quartz stockwork (silica flooding of the rocks) exposed at the surface in the center of the area. Skarn, composed mainly of brown andradite garnet

intergrown with calcite, epidote, and tremolite, occurs around the perimeter of the quartz monzonite stock in Precambrian rocks. The NGM area has many of the characteristics common to porphyry copper deposits, however, there has not been any secondary (supergene) enrichment, and thus economic concentrations of ore do not occur. Complexly faulted, Tertiary volcanic rocks related to the Timber Mountain Caldera in southern Nevada are abundant around the southern periphery of the study area and are overlain by volcaniclastic sedimentary rocks interbedded with rhyolite and basalt (Wrucke et al., 1984). Quaternary deposits include Holocene and Pleistocene fanglomerates, pediment gravels, and alluvium; these have been mapped in reconnaissance (Moring, 1986) but no linked bedrock/surficial geology studies have been completed.

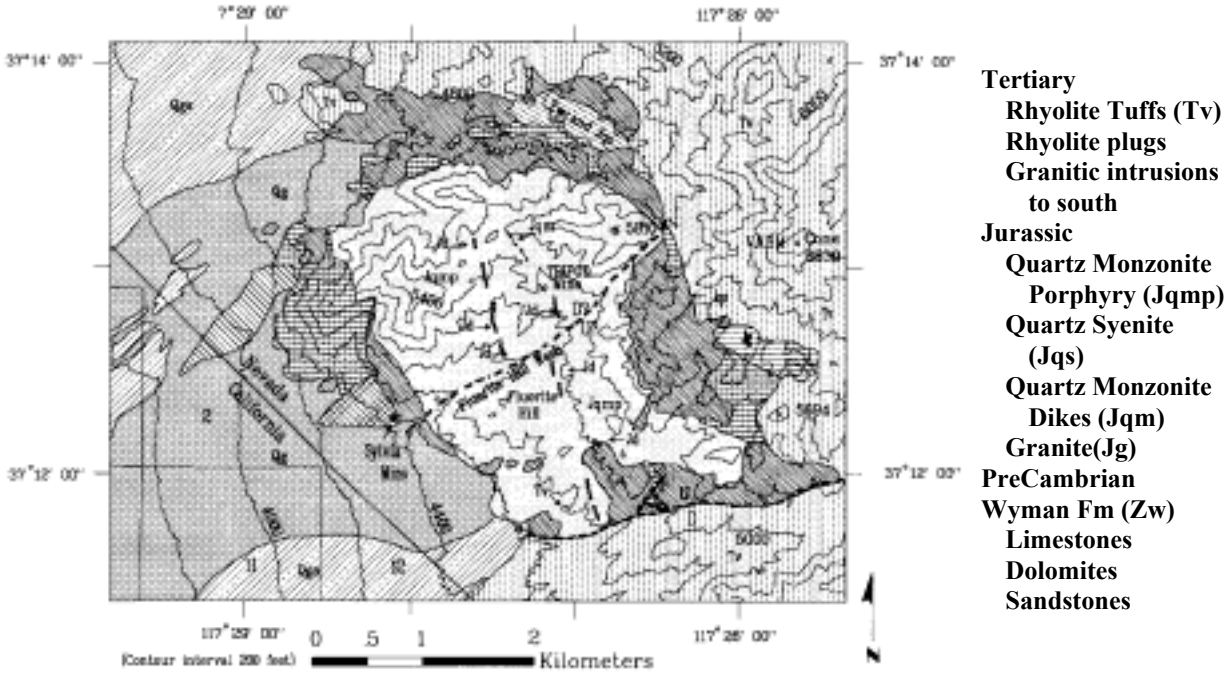

Figure 2: Geologic Map of the NGM Site

3.0 FIFTEEN YEARS OF HYPERSPECTRAL SENSING

A variety of hyperspectral sensors were flown over the northern Grapevine Mountains site from 1982 through 1998. The following sections describe the data characteristics, analysis methods, and results for these sensors.

3.1 GER Spectral Profiler (1982)

The Geophysical Environmental Research Spectroradiometer (GERS) was an aircraft, non-imaging, spectral profiler (Collins et al., 1981) that collected data between 1.96 and 2.5μm in 64 contiguous, 8.6 nanometer-wide channels. A complete spectrum was measured with a 20 meter GFOV at 20 meter intervals along the flightline. Fifteen flightlines of GERS data (approximately 3,500 spectra) were acquired for the northern Grapevine Mountains site during 1982, and color photographs acquired during the flight allowed compilation of a flightline map (Figure 3). The contributions of the atmosphere and the solar spectrum were removed using the IAR Reflectance method (a variation on the Flat Field method, Kruse, 1988) to get to reflectance spectra similar to laboratory measurements (Figure 4). The GERS data were analyzed by extracting individual spectra, preparing stacked spectra images, and along-flightline profiles of the data (Figure 5). Figure 6 shows the interpreted mineralogy overlain on the flightline map and topography (and interpolated between flightlines). The GERS allowed identification of individual minerals and mapping of the general distribution of surface materials. Targets were identified for more detailed study that were not identified in the previous Landsat analysis and subsequent field reconnaissance. The GERS data and basic analysis techniques developed served to demonstrate the utility of high quality aircraft spectrometer data for mineralogical mapping. The results provided sufficient new information that USGS became involved in the NASA Airborne Imaging Spectrometer (AIS) program.

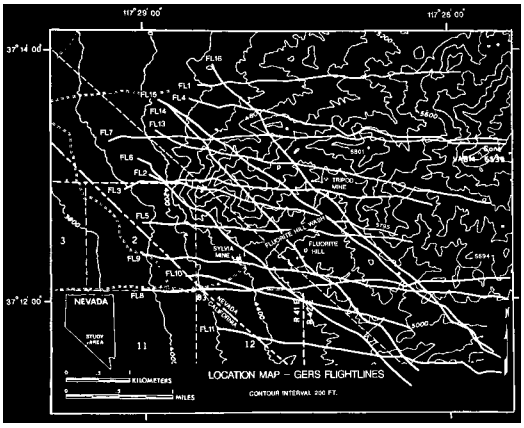

Figure 3: GERS Flightline map for NGM.

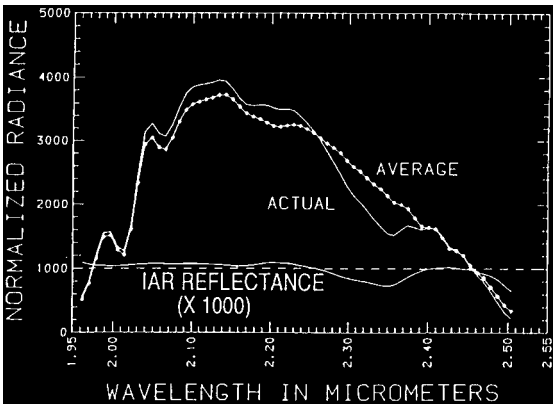

Figure 4: IAR Reflectance for GERS data

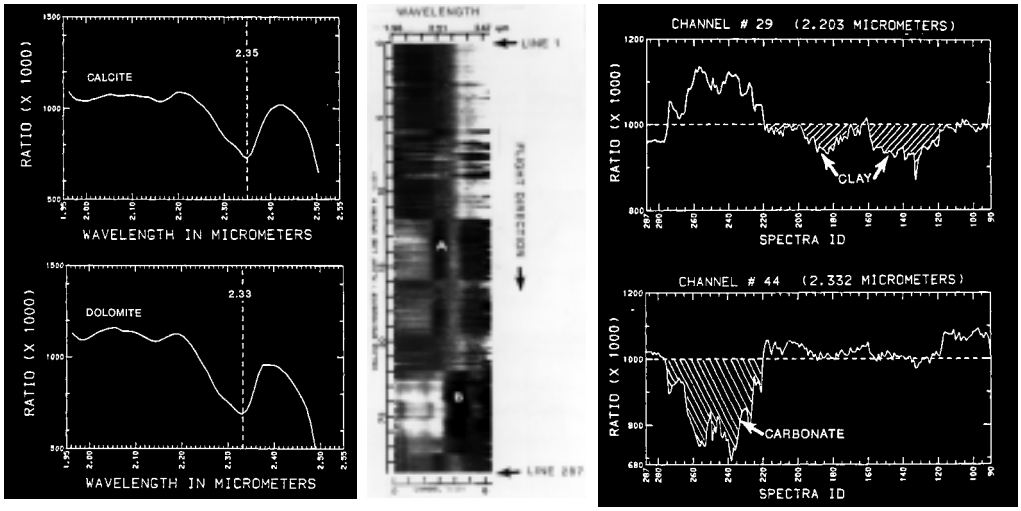

Figure 5: GER spectral plots, stacked grayscale spectra, and flightline profiles for flightline 6 (FL6).

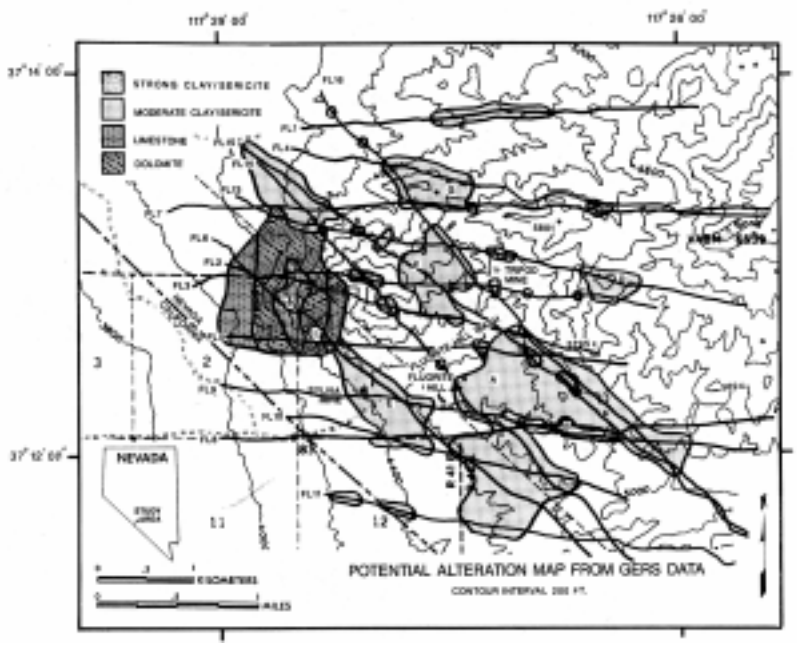

Figure 6: GER Spectral Profiler Interpreted Mineralogy

3.2 Airborne Imaging Spectrometer (AIS) (1984 - 1986)

The Airborne Imaging Spectrometer (AIS) was similar to the GERS in spectral resolution (9.3nm cf. 8.6nm) and spatial resolution (10 to 15m cf. 20m) but unlike the GERS the AIS was designed specifically as an imaging device. The AIS was an experimental sensor designed to test two dimensional, near-infrared area array detectors. This instrument imaged 32 (AIS-1, 1983-1985) or 64 (AIS-2, 1986) cross-track pixels simultaneously, collecting data in 128 contiguous narrow (AIS-1 [9.3nm], AIS-2 [10.6nm]) channels from approximately 1.2 to 2.5μm (Vane et al.,1983; Goetz et al., 1985; Vane, 1986). The AIS-1 was flown on a NASA C-130 aircraft at an altitude of approximately 4,500 meters above mean terrain, resulting in an average ground pixel size of about 10.9 X 10.9 meters and a swath width of about 350 meters. The AIS-2 was flown at a similar altitude, but the revised instrument characteristics resulted in an average ground pixel of about 14.4 X 14.4 meters and swath width of about 920 meters. Locations of the 1984 through 1986 NGM AIS data registered to a topographic map are shown in Figure 7.

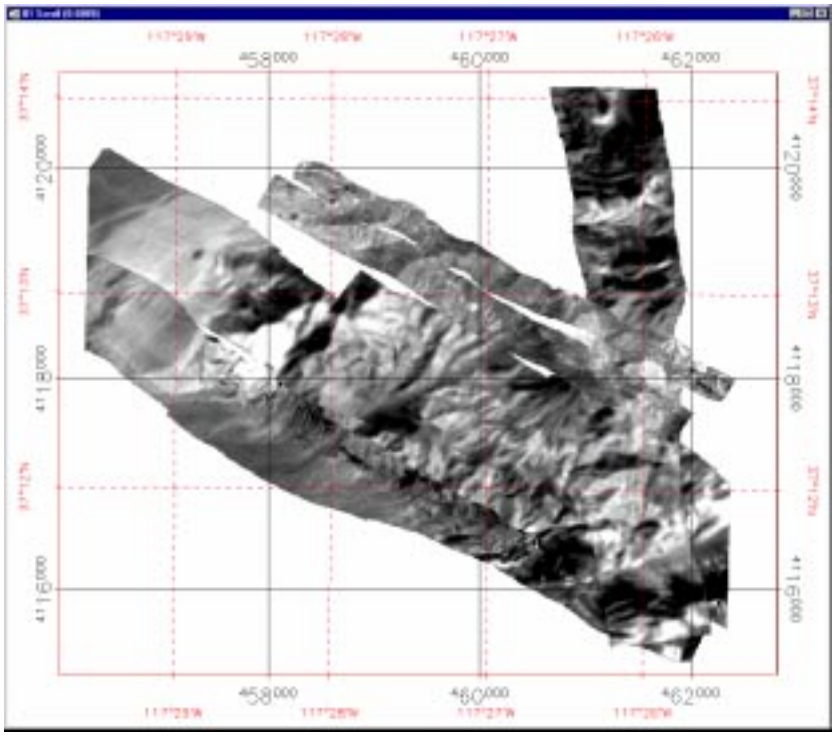

Figure 7: AIG Flightlines at NGM 1984 – 1986.

The AIS data were calibrated to apparent reflectance using the IAR Reflectance technique (Kruse, 1988). Selected reflectance spectra for 1984 through 1986 data at the NGM site are shown in Figure 8. Algorithms were developed to identify automatically the strongest absorption feature in the 2.1 to 2.4 μm portion of each AIS spectrum. Removal of a continuum (Clark and Roush, 1984) was used to place all of the absorption features on a common reference plane. The continuum was calculated using a second order polynomial fitted to selected channels (channels without absorption features) in the relative reflectance spectra. The continuum then was "removed" by dividing the polynomial function into the actual data. A color image showing absorption band information was designed using an intensity, hue, saturation (IHS or "Munsell") color transform (Raines, 1977; Kruse and Raines, 1984; Kruse et al., 1986) to map the three band parameters band position, band depth, and band asymmetry into red, green, blue (RGB) color space. The band depth was mapped into intensity, the band width was mapped into saturation, and the band position was mapped into hue. Transformation of the IHS-encoded spectral information into the RGB color space produced an image in which all of the absorption band information for the strongest absorption feature in each pixel

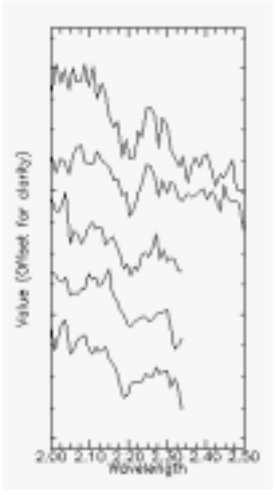

Figure 8: AIS Spectra of Sericite

image colors. The registered AIS images and spectra were used to identify areas for further detailed investigation. Individual spectra and groups of spectra were extracted from the AIS data and comparisons were made to absorption band parameters extracted from spectra of laboratory standards and to published spectra to identify alteration minerals. An interpretive map of the NGM site mineralogy using the AIS data is shown in Figure 9.

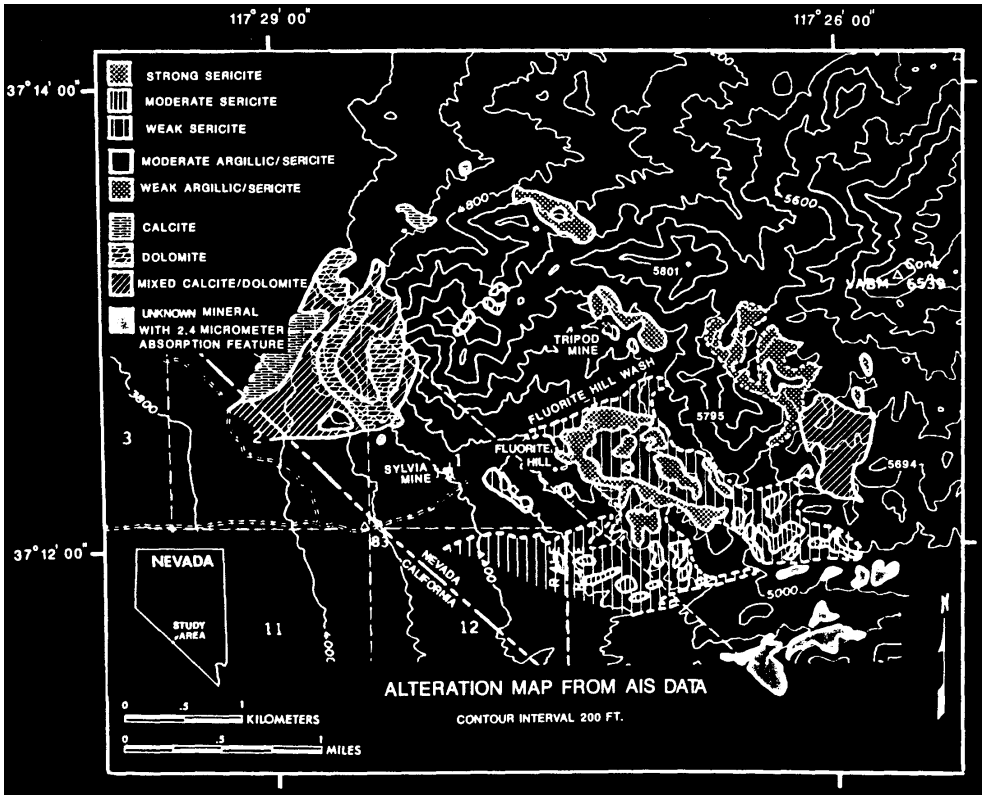

Figure 9: Interpreted NGM alteration mineralogy from AIS data.

The AIS alteration map was field checked during 1986 and generally shows good correspondence with field mapping. Two types of alteration were mapped with the AIS data and subtle differences in surficial mineralogy were observed. Areas of sericite alteration could be identified based upon a strong absorption feature near 2.21 μm, a weak shoulder near 2.25 μm, a weak absorption band near 2.35 μm and an additional weak band near 2.44 μm. In one area of weakly sericitized rock, X-ray diffraction analysis demonstrated that the predominant soil clay mineral was montmorillonite. Although this soil contained less sericite than montmorillonite, the spectral character of the sericite dominated the near-infrared spectra and montmorillonite was not identified using field, laboratory, or aircraft spectra; X-ray diffraction was required to identify the montmorillonite. Areas of argillic alteration were identified by the presence of a weak to moderate absorption feature near 2.21 μm caused by montmorillonite; identification of montmorillonite was possible only when no masking minerals (such as sericite) were present. Calcite and dolomite were identified based on a sharp absorption feature near 2.34 and 2.32 μm, respectively, and other weak absorption features that are at shorter wavelengths in the dolomite spectra than in the calcite spectra. Fan gravels derived from both dolomite and limestone bedrock have shallow, broad absorption bands near 2.34 μm; these bands resemble those for calcite rather than dolomite. The position of the absorption feature in the fan gravels (near 2.34 μm regardless of provenance), may be caused by a shift towards calcite composition in the development of soil. Isolated spectra having some characteristics of skarn minerals, such as epidote, tremolite, and actinolite, were observed in the AIS data but could not be confirmed independently. An unknown 2.4 μm mineral (later field/lab verified as Zeolite) was also mapped using the AIS data.

3.3 Airborne Visible/Infrared Imaging Spectrometer (AVIRIS) (1987 - 1994)

The Airborne Visible/Infrared Imaging Spectrometer (AVIRIS) became operational in 1987. AVIRIS measures near-laboratory-quality spectra in 224 10 nm-wide channels in the spectral range 0.41 to 2.45 μm (Porter and Enmark, 1987). From 1987 – 1998, AVIRIS was flown aboard the NASA ER-2 aircraft at an altitude of 20 km, with an instantaneous field of view of 20 m and a swath width of about 10 km.

AVIRIS data for the NGM site were initially obtained during May 1987, however, with very poor signal-to-noise performance. After enhancements to the instrument, data were again acquired in 1989 with signal-to-noise ratios of approximately 50/1 at 0.70 μm and 20/1 at 2.20 μm for targets with reflectances of 0.5 (Kruse, unpublished data). The Spectral Image Processing System (SIPS) (Kruse et al., 1993b) was used to preview the AVIRIS radiance images and to extract image radiance spectra for calibration. The data were calibrated to apparent reflectance using ground targets and the empirical line method (Ballew, 1975, Roberts et al, 1985; Kruse et al., 1993a). Once the data were calibrated to reflectance, interactive analysis using SIPS was used to determine the principal minerals at the surface. Extraction of average spectra from areas with spectral character allowed comparison to library spectra of specific minerals for identification. A simple, commonly used method for analysis of imaging spectrometer data, binary encoding and spectral matching using a reference library (Mazer et al, 1988) was used to make mineral maps. The binary encoding method was selected for analysis of the 1989 AVIRIS data because it is robust in the presence of noise. Laboratory spectra for calcite, dolomite, illite (sericite), hematite, and goethite were used as references for the classification. The 2.0 - 2.4 μm region was selectively used for the carbonates and sericite, while the 0.4 - 1.0 μm range was used for the iron oxide minerals. These regions were chosen for encoding because of observed diagnostic spectral characteristics limited to these wavelength ranges of the spectrum. Selected examples comparing Fe Oxide spectra from the AVIRIS data to those in the spectral library are shown in Figure 9. Analysis results for these data have been published in Kruse et al., 1993a.

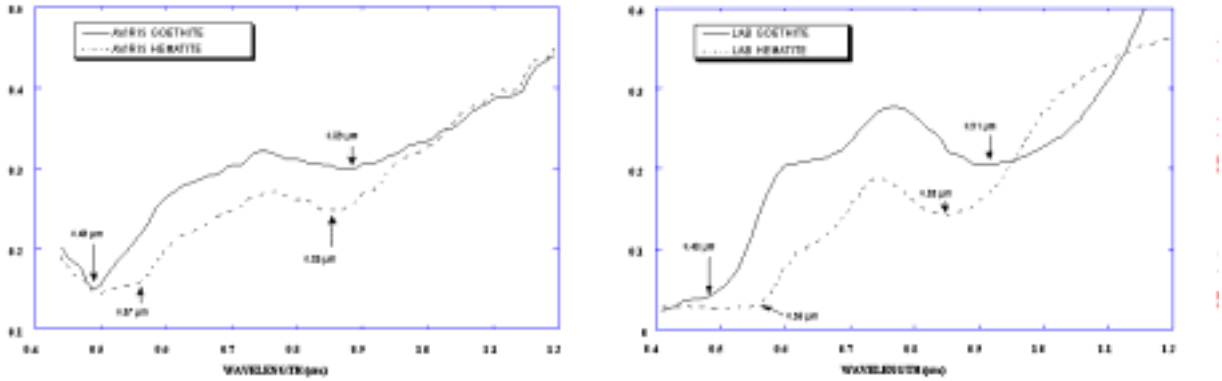

Figure 10: AVIRIS spectra for Hematite and Goethite compared to laboratory spectra

Additional AVIRIS datasets were acquired in 1992, 1994, and 1995. As the sensor matured, SNR improved, and new analysis methods became available, additional detailed mapping was possible. Spectral Angle Mapper (SAM) (Kruse et al., 1993b; Boardman, unpublished data), an expert system approach (Kruse et al., 1993a), and spectral unmixing (Boardman, 1989, 1993) were applied to 1992 and 1994 data. SAM produced convincing results, however, the exact mineralogy displayed is highly dependent on arbitrary thresholds set by the user. The expert system provided a means of matching specific spectral features using continuum-removal and feature extraction algorithms and a basic set of rules derived from the analysis of laboratory spectra (Kruse, 1993a). The expert system approach, however, requires SNRs of approximately 50/1 or better to achieve success rates of 95% (Kruse, unpublished data). The output of the expert system analysis is a "continuum-removed" cube with 224 bands containing all of the continuum-removed spectra calculated from the reflectance data, a "feature" cube containing the wavelength positions, depths, FWHMs, and asymmetries for each pixel for the ten strongest absorption features, and an "analysis cube" showing the location and probability of occurrence of the materials in the library. A "final decision best endmember" image was also produced showing the single best match for each pixel. Linear spectral unmixing using the endmember spectra for calcite, dolomite, sericite, hematite, and goethite produced an image data cube with the same spatial dimensions as the input data; five spatial output bands representing the abundances of the five endmembers (Boardman, 1989, 1993). The analysis also produced two additional images, one showing the sum of the abundances at each pixel, and the other the root-mean-square (rms) error values at each pixel.

Analysis of the 1989 – 1994 AVIRIS confirmed and refined the zoned alteration patterns at the NGM site, including the predominance of quartz-sericite-pyrite alteration. The AVIRIS data confirmed separation of calcite and dolomite based on a 10 nm band position shift and allowed identification of some skarn mineralization as well as confiming zeolite identification and distribution. AVIRIS data also showed that goethite is generally associated with intruded, altered rocks and with Ag-bearing veins, while hematite is generally associated with later volcanic rocks. The 1992 and 1994 data also confirmed that several sericite (muscovite) endmembers exist and allowed expansion of the study to a larger area.

3.4 Airborne Visible/Infrared Imaging Spectrometer (AVIRIS) (1995)

AVIRIS data collected in 1995 achieved new levels of performance and very high SNR (Green et al. 1996). As a result, this stimulated new developments in atmospheric correction capabilities and analysis methodologies. Boardman and Kruse, 1994, Boardman et al., 1995; and Kruse et al., 1996 summarize a comprehensive methodology for analyzing hyperspectral data. These methods rely on atmospherically corrected data and concentrate on finding the key endmember spectra defined by the data space, identifying them, mapping their spatial distributions, and quantifying abundances for each pixel (Figure 11). This methodology is implemented in the commercial software system "ENVI®", the Environment for Visualizing Images.

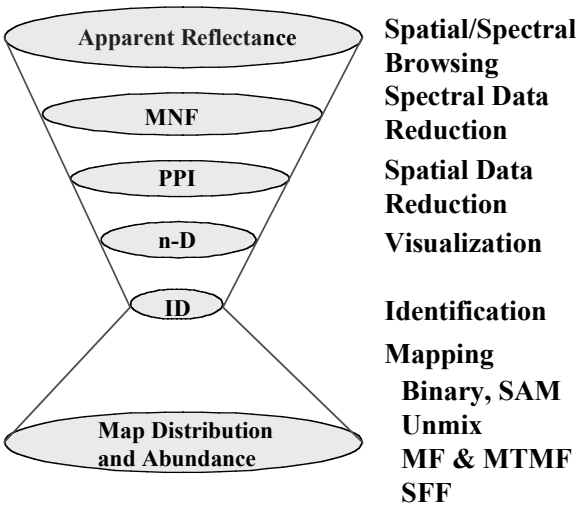

Figure 11: Hyperspectral-based method of endmember determination, identification, mapping, and quantification

The 1995 NGM AVIRIS data were analyzed using these methods. The data were processed to apparent reflectance using the ATREM software (Gao and Goetz, 1990). ATREM is an atmospheric model-based routine that converts the calibrated radiance measured by the sensor to apparent surface reflectance without requiring in-situ measurements (CSES, 1992). The spectral data volume was reduced using the Minimum Noise Fraction (MNF) transformation (Green et al., 1988), the spatial data volume was reduced using the Pixel Purity Index™ (PPI) (Boardman et al., 1995). The N-Dimensional Visualizer™ was used to determine image endmembers (Boardman, 1993; Boardman et al., 1995). Identification of endmembers was accomplished using their reflectance spectra and the Spectral Analyst™ (Kruse et al., 1993a; Kruse and Lefkoff, 1993), and mineral mapping done using several methods including SAM, linear spectral unmixing and matched filtering (Kruse et al., 1993b; Boardman, 1989, 1993, 1993; Boardman and Kruse, 1994; Harsanyi and Chang, 1994) and also outlined in Kruse et al. (1996).

Operationally, the AVIRIS data were linearly transformed using the MNF transformation, and the top MNF bands, which contain most of the spectral information, were used to determine the most likely endmembers using the PPI procedure. These potential endmember spectra were loaded into an n-dimensional scatterplot and rotated in real time on the computer screen until "points" or extremities on the scatterplot were exposed. These projections were "painted" using Region-of-Interest (ROI) definition procedures and then rotated again in 3 or more dimensions (3 or more bands) to determine if their signatures were unique in the AVIRIS MNF data. Once a set of unique pixels were defined, then each separate projection on the scatterplot (corresponding to a pure endmember) was exported to

® ENVI is a Registered Trademark of BSCLLC, Lafayette, Colorado.

a ROI in the image. Mean spectra were then extracted for each ROI from the apparent reflectance data to act as endmembers for spectral mapping. These endmembers or a subset of these endmembers were used for subsequent classification and other processing. The Spectral Angle Mapper (SAM), Linear Spectral Unmixing, and Matched filtering were used to produce mineral maps. The results are generally presented as gray-scale images with values from 0 to 1.0, which provide a means of estimating mineral abundance. Brighter pixels in the images represent higher mineral abundances. Figure 12 shows several of the endmember spectra extracted from the data and selected endmember abundance mapping results.

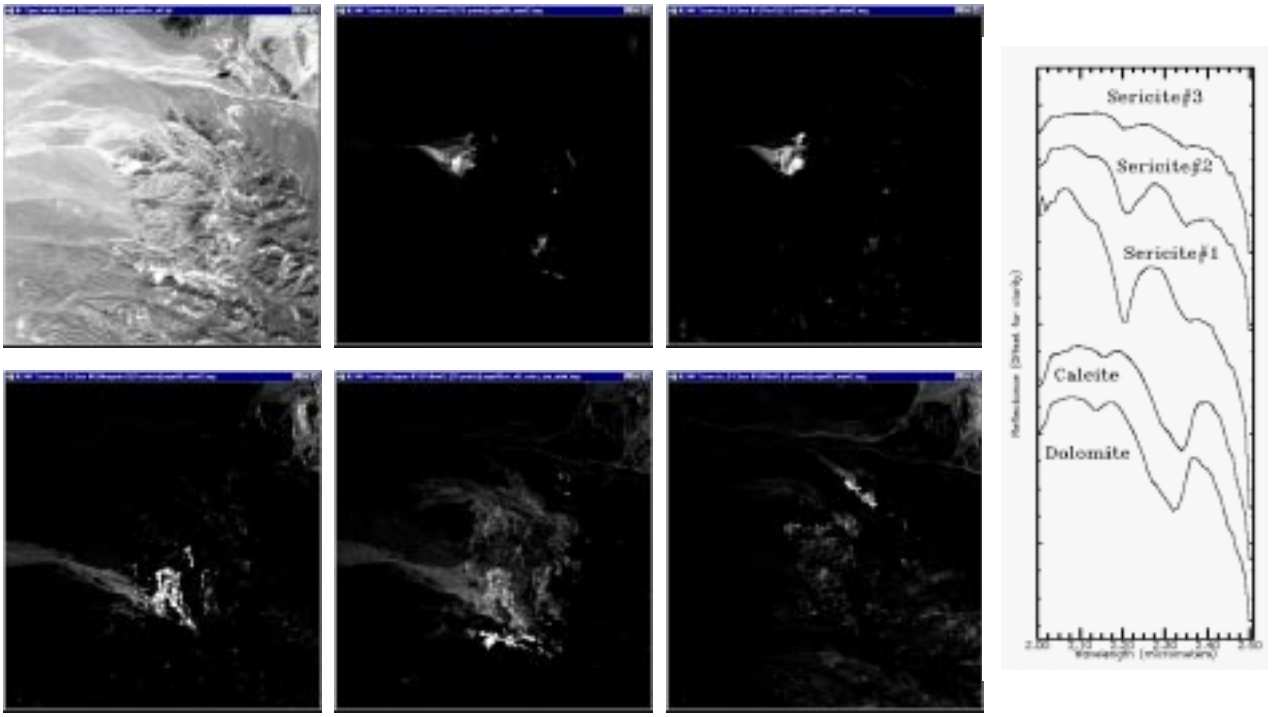

Figure 12: Matched filtering results for the NGM site. Upper left image is 0.67 μm image band. Abundance images clockwise from the top center image are 1) Calcite, 2) Dolomite, 3) Sericite #1, 4) Sericite #2, 5) Sericite #3. The plot on the right side of the figure shows selected endmember spectra.

The ability to map materials at the sub-pixel level was clearly established with the 1995 AVIRIS data. Several areas of subpixel dolomite occurrence were selected from the 1995 results for field checking. Boardman and Kruse located these subpixel occurrences in the field, and verified their mineralogy using a field spectrometer. Figure 13 shows two sub-pixel outcrops of dolomite at the approximately 1% and 3% levels respectively.

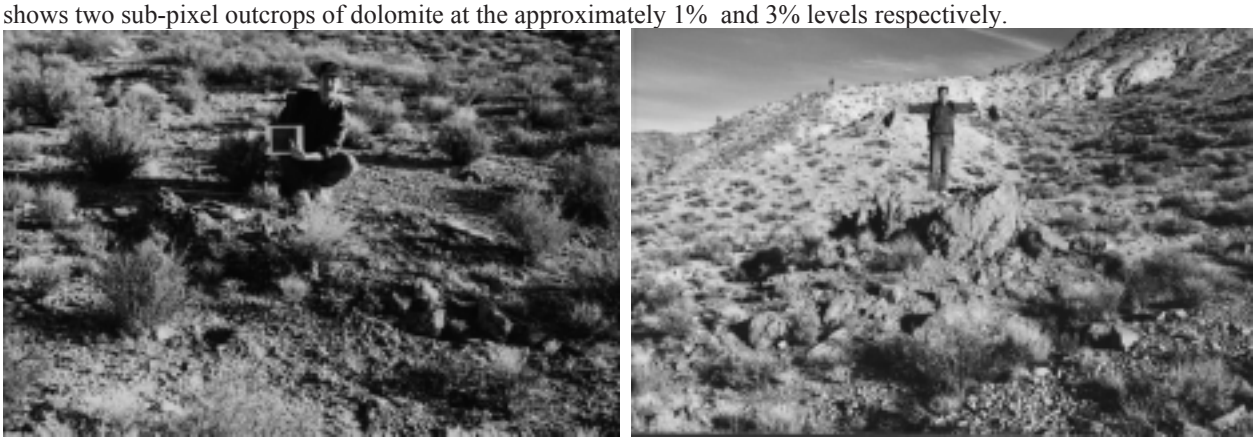

Figure 13: Field verification of spectral mixing results. Left photo shows an approximately 1 x 3 meter outcrop of dolomite found using sub-pixel detection. Right photo shows approximately 3 x 3 meter outcrop of dolomite.

The 1995 AVIRIS data and new processing methods confirmed and refined the separation of calcite and dolomite using only hyperspectral reflectance data. Mapping of sub-pixel occurrences of dolomite was possible at the 1% level in a contrasting background of igneous rocks. The AVIRIS data were also used to demonstrate identification of several different sericite (muscovite) endmembers. Microprobe analysis by CSIRO shows that sericites with shorter wavelength absorption features near 2.2 μm have higher aluminum in octahedral coordination, while those with higher wavelength features near 2.2 μm have significant substitution of Fe and Mg in octahedral sites.

3.5 Low Altitude AVIRIS (1998)

The AVIRIS sensor was flown over the NGM site on a twin Otter aircraft at low altitude during October 1998 as part of NASA/JPL's low altitude AVIRIS test project (Chrien et al., 1999; Green et al., 1999). The data were corrected to ~2.4 meter pixels using on board navigation and GPS (Boardman, 1999). The 1998 AVIRIS data were processed using the standardized AIG methodologies described above. Figure 14 shows selected spectra extracted from the data.

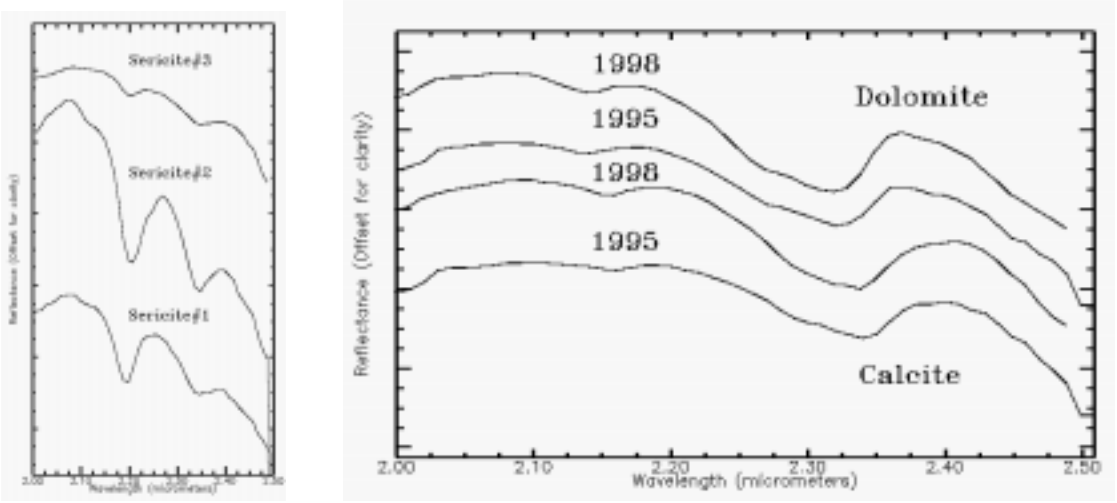

Figure 14: Selected 1998 AVIRIS spectra and 1998 AVIRIS spectra compared to 1995 AVIRIS spectra

AVIRIS data collected on the low altitude platform provide high spectral resolution, high-quality spectra at very high spatial resolution. The 1998 AVIRIS confirms and refines previous AVIRIS identifications and mapping and validates endmembers for similar coverage. The high spatial resolution resolves fine geologic detail not visible in the high-altitude AVIRIS data. Figure 15 shows a comparison of high- (~20m pixel) and low-altitude (~2.4m pixel) AVIRIS data for the main part of the altered system at the NGM site.

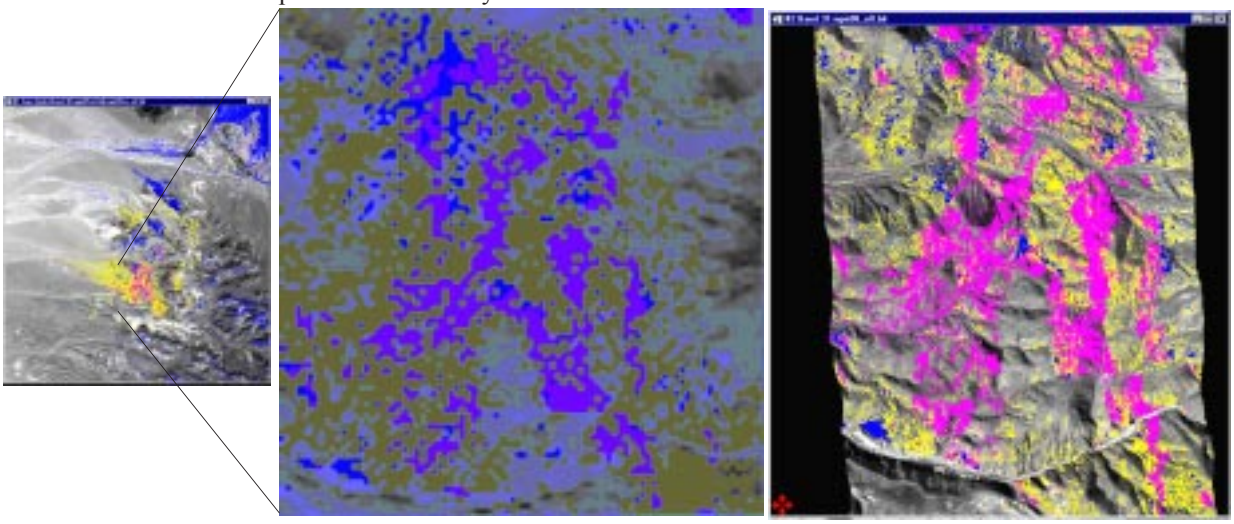

Figure 15: Comparison of high-altitude 1995 results to low-altitude 1998 results for three sericite species for the central part of the alteration system. Note similar spatial patterns, but higher detail shown in 1998 AVIRIS.

4.0 SUMMARY AND CONCLUSIONS

A summary of hyperspectral sensing and processing from 1982 – 1998 at the northern Grapevine Mountains, Nevada, site serves to illustrate the advances made in sensor systems and analysis algorithms over 15 years. Availability of high quality reflectance spectra for mapping began with the GERS spectral line profiler. This instrument produced data with an excellent SNR that demonstrated the potential of the technology. The AIS system, an area-array imaging spectrometer, provided the first hyperspectral images of the NGM area, but detector and software limitations made analysis of these data difficult and lack of complete spatial coverage prevented full understanding of the hydrothermal system. Good-quality AVIRIS data became available in 1989 and were subsequently acquired in 1992, 1994, and 1995. Each improvement to the sensor required that additional analysis techniques be developed and each improvement in the algorithms spurred further sensor improvements. The net result of repeat acquisitions at this site and others was that AVIRIS became an operational system capable of producing detailed geologic and alteration maps that could not be obtained by any other means.

At the reconnaissance level, 1995 and high spatial resolution 1998 AVIRIS produce similar results. The major minerals were detected and mapped at both ~20 and 2.4 m spatial resolution. The major benefit of the 1998 AVIRIS, with 2.4 meter spatial resolution, is that it allows mapping of greater detail at the "deposit" level. Spatial resolution has been increased significantly without any apparent effect on SNR or spectral performance. The only real impact is on spatial coverage and level of detail. The AVIRIS hyperspectral system has now progressed to the state where it can be used to produce laboratory quality spectra without any ground measurements. With the 1998 implementation of fully geocorrected AVIRIS data, analysis results are readily available in map form, making aircraft hyperspectral data a viable mapping option.

The combination of field mapped geologic and alteration maps, hyperspectral remote sensing results, and other data sets at the NGM site show structural control of intrusions and alteration. Field work confirms the distribution of carbonates mapped using the hyperspectral systems and multiple sericite/muscovite endmembers and distribution. The hydrothermal system at NGM has many of the elements of a Porphyry Cu/Mo system, however, no supergene enrichment is present, thus it is a non-economic occurrence. The site remains ideal for continued verification and refinement of remote sensing technology.

5.0 ACKNOWLEDGEMENTS

This research was supported over the years by the U.S. Geological Survey, Colorado School of Mines, NASA/JPL, and Analytical Imaging and Geophysics LLC. Special thanks are due to the JPL AVIRIS team for their dedication and support.

6.0 REFERENCES CITED

Albers, J. P., and Stewart, J. H., 1972, Geology and mineral deposits of Esmeralda County, Nevada: Nevada Bureau of Mines and Geology Bulletin 78, 80 p.

Ballew, G., 1975, A method for converting Landsat I MSS data to reflectance by means of ground calibration sites: Stanford Remote Sensing Laboratory Technical Report 75-5, Stanford, CA.

Boardman, J. W., 1989, Inversion of imaging spectrometry data using singular value decomposition: in Proceedings, IGARSS '89, 12th Canadian Symposium on Remote Sensing, 4, pp. 2069-2072.

Boardman, J. W., 1993, Automated spectral unmixing of AVIRIS data using convex geometry concepts: in Summaries, Fourth JPL Airborne Geoscience Workshop, JPL Publication 93-26, v. 1, p. 11 - 14.

Boardman, J. W., 1999, Precision geocoding of AVIRIS low-altitude data: lessons learned in 1998: in Proceedings of the 8th JPL Airborne Earth Science Workshop: Jet Propulsion Laboratory Publication (in press).

Boardman, J. W., and Kruse, F. A., 1994, Automated spectral analysis: A geological example using AVIRIS data, northern Grapevine Mountains, Nevada: in Proceedings, Tenth Thematic Conference, Geologic Remote Sensing, 9-12 May 1994, San Antonio, Texas, p. I-407 - I-418.

Boardman, J. W., Kruse, F. A., and Green, R. O., 1995, Mapping target signatures via partial unmixing of AVIRIS data: in Summaries, Fifth JPL Airborne Earth Science Workshop, JPL Publication 95-1, v. 1, p. 23-26.

Clark, R. N., and Roush, T. L., 1984, Reflectance spectroscopy: Quantitative analysis techniques for remote sensing applications: Journal of Geophysical Research, v. 89, no. B7, pp. 6329-6340.

Center for the Study of Earth from Space (CSES), 1992, "ATmosphere REMoval Program (ATREM), Version 1.1." Internal Report, University of Colorado, Boulder: 24 p

Chrien, T. G., Green, R. O., Boardman, J. W., Chippendale, B., Chovit, C. J., Eastwood, M., Faust, J. A., Finn, M., Hall, P., Holbrook, J., Houston, J., Kurzweil, c., Longenecker, J., Raney, J., Sarture, C., and Tuell, G., 1999, Operation of NASA's Airborne Visible/Infrared Imaging Spectrometer (AVIRIS) on a NOAA Twin Otter: Program Review: in Proceedings of the 8th JPL Airborne Earth Science Workshop: Jet Propulsion Laboratory Publication (in press).

Collins, William, Chang, S.H., Kuo, J.T., and Rowan, L.C., 1981, Remote mineralogical analysis using a high-resolution spectrometer: Preliminary results of the Mark II system: IEEE, International Geoscience and Remote Sensing Symposium, Washington, D. C., Digest, v. 1, p. 327-334.

Gao B. and Goetz, A. F. H. (1990). "Column atmospheric water vapor and vegetation liquid water retrievals from airborne imaging spectrometer data." Journal of Geophysical Research, 95(D-4): p. 3549-3564.

Goetz, A. F. H., Vane, G., Solomon, J. E., and Rock, B. N., 1985, Imaging spectrometry for earth remote sensing: Science, 228, 1147-1153.

Green, A. A., Berman, M., Switzer, B., and Craig, M. D., 1988, A transformation for ordering multispectral data in terms of image quality with implications for noise removal: IEEE Transactions on Geoscience and Remote Sensing, v. 26, no. 1, p. 65 - 74.

Green, R. O., Conel, J. E., Margolis, J., Chovit, C., and Faust, J., 1996, In flight calibrtion and validation of the Airborne Visible/Infrared Imaging Spectrometer (AVIRIS): in Proceedings, 6th Airborne Visible/Infrared Imaging Spectrometer (AVIRIS) workshop, JPL Publication 96-4, v. 1, p. 115 - 126.

Green, R. O., Pavri, B., Faust, J., Chovit, C., and Williams, O., 1999, AVIRIS in-flight radiometric calibration results for 1998: in Proceedings of the 8th JPL Airborne Earth Science Workshop: Jet Propulsion Laboratory Publication (in press).

Kruse, F. A., 1987, Use of high spectral resolution remote sensing to characterize weathered surfaces of hydrothermally altered rocks: Unpublished Ph. D. dissertation, Colorado School of Mines, Golden, 139 p.

Kruse, F. A., 1988, Use of Airborne Imaging Spectrometer data to map minerals associated with hydrothermally altered rocks in the northern Grapevine Mountains, Nevada and California: Remote Sensing of Environment, v. 24, no. 1, pp. 31-51.

Kruse, F. A., and Lefkoff, A. B., 1993, Knowledge-based geologic mapping with imaging spectrometers: Remote Sensing Reviews, Special Issue on NASA Innovative Research Program (IRP) results, v. 8, p. 3 - 28.

Kruse, F. A., and Raines, G.L., 1984, A technique for enhancing digital color images by contrast stretching in Munsell color space: in Proceedings, International Symposium on Remote sensing of Environment, Third Thematic Conference, "Remote Sensing for Exploration Geology", Colorado Springs, 16-19 April 1984, Ann Arbor, Environmental Research Institute of Michigan, p. 755-760.

Kruse, F. A., Huntington, J. H., and Green, R. O, 1996, "Results from the 1995 AVIRIS Geology Group Shoot." In Proceedings, 2nd International Airborne Remote Sensing Conference and Exhibition, I: p. I-211 - I-220.

Kruse, F. A., Knepper, D. H. Jr., and Clark, R. N., 1986, Use of digital Munsell color space to assist interpretation of imaging spectrometer data -- Geologic examples from the northern Grapevine Mountains, California and Nevada: in Proceedings, 2nd AIS Data Analysis Workshop, Pasadena, California 6-8 May, l986, JPL Publication 86-35, Jet Propulsion Laboratory, Pasadena, California, p. 132-137.

Kruse, F. A., Lefkoff, A. B., and Dietz, J. B., 1993a, Expert System-Based Mineral Mapping in northern Death Valley, California/Nevada using the Airborne Visible/Infrared Imaging Spectrometer (AVIRIS): Remote Sensing of Environment, Special issue on AVIRIS, May-June 1993, v. 44, p. 309 - 336.

Kruse, F. A., Lefkoff, A. B., Boardman, J. B., Heidebrecht, K. B., Shapiro, A. T., Barloon, P. J., and Goetz, A. F. H., 1993b, The Spectral Image Processing System (SIPS) - Interactive Visualization and Analysis of Imaging Spectrometer Data: Remote Sensing of Environment, Special issue on AVIRIS, May-June 1993, v. 44, p. 145 - 163.

Mazer, A. S., Martin, M., Lee, M., and Solomon, J. E., 1988, Image processing software for imaging spectrometry data analysis: Remote Sensing of Environment, v. 24, no. 1, pp. 201-210.

Moring, B., 1986, Reconnaissance surficial geologic map of northern Death Valley, California and Nevada: U. S. Geological Survey Miscellaneous Field Studies Map MF-1770, 1:62,500, 1 sheet.

Porter, W. M., and Enmark, H. T., 1987 A system overview of the Airborne Visible/Infrared Imaging Spectrometer (AVIRIS): in Proceedings, 31st Annual International Technical Symposium, Society of Photo-Optical Instrumentation Engineers, v. 834, pp. 22-31.

Raines, G. L., 1977, Digital color analysis of color ratio composite Landsat scenes: in Proceedings, Eleventh International Symposium on Remote Sensing of Environment, University of Michigan, Ann Arbor, p. 1463-1472.

Roberts, D. A., Yamaguchi, Y., and Lyon, R. J. P. (1985), Calibration of Airborne Imaging Spectrometer Data to percent reflectance using field spectral measurements: in Proceedings, Nineteenth International Symposium on Remote Sensing of Environment, Ann Arbor, Michigan, October 21-25, 1985.

Vane, Gregg, Goetz, A. F. H., and Wellman, 1983, Airborne Imaging Spectrometer: A New Tool for Remote Sensing: Proceedings IEEE 1983 International Geoscience and Remote Sensing Symposium, IEEE Cat. No. 83CH1837-4.

Vane, Gregg, 1986, Introduction to the proceedings of the second Airborne Imaging Spectrometer (AIS) data analysis workshop: in Vane, Gregg, and Goetz, A.F.H. eds., Proceedings of the Second Airborne Imaging Spectrometer Data Analysis Workshop, JPL Publication 86-35, Jet Propulsion Laboratory, Pasadena, California, p. 1-16.

Wrucke, C. T., Werschkey, R. S., Raines, G. L., Blakely, R. J., Hoover, D. B, and Miller, M. S., 1984, Mineral resources and mineral resource potential of the Little Sand Spring Wilderness Study Area, Inyo County, California: U. S. Geological Survey Open File Report 84-557, 20 p.